ADVANCED BIOSYSTEMS
www.adv-biosys.com

# Conducting Polymer Scaffolds for Hosting and Monitoring 3D Cell Culture

*Sahika Inal,* Adel Hama, Magali Ferro, Charalampos Pitsalidis, Julie Oziat, Donata Iandolo, Anna-Maria Pappa, Mikhael Hadida, Miriam Huerta, David Marchat, Pascal Mailley, and Róisín M. Owens**

**This work reports the design of a live-cell monitoring platform based on a macroporous scaffold of a conducting polymer, poly(3,4-ethylene dioxythiophene):poly(styrenesulfonate). The conducting polymer scaffolds support 3D cell cultures due to their biocompatibility and tissue-like elasticity, which can be manipulated by inclusion of biopolymers such as collagen. Integration of a media perfusion tube inside the scaffold enables homogenous cell spreading and fluid transport throughout the scaffold, ensuring long term cell viability. This also allows for co-culture of multiple cell types inside the scaffold. The inclusion of cells within the porous architecture affects the impedance of the electrically conducting polymer network and, thus, is utilized as an in situ tool to monitor cell growth. Therefore, while being an integral part of the 3D tissue, the conducting polymer is an active component, enhancing the tissue function, and forming the basis for a bioelectronic device with integrated sensing capability.**

## 1. Introduction

Advances in tissue engineering have demonstrated that physical architecture of tissues is extremely important for correct differentiation, and that a wealth of factors are important to correctly model tissues in vitro.[1,2] It is now well accepted that the in vivo environment, comprising both the composition (different cell types, extracellular matrix (ECM) etc.), as well as the 3D structure, can have a tremendous influence on the function and differentiation of the cells.[3] 2D (or flat biology) approaches often result in loss of phenotypes due to dissociation from the native environment followed by propagation on flat, impermeable substrates preventing cells from being responsive to chemical and biochemical gradients naturally found in vivo.[4] It is now clear that architectures that reproduce tissue organization in 3D are favored for studying function as first shown by Bissell and co-workers nearly 30 years ago.[5,6] Another emerging concept is the capacity for multiple cell types to auto-organize when given the appropriate mechanical cues.[7] A large variety of 3D models have been developed, with the major subtypes being spheroids/organoids, multilayered tissue like models, and scaffold models.[8] 3D tissues are frequently constructed as spheroids using hydrogel-like matrices such as Matrigel,[9] or PuraMatrix,[10] with a highly desirable degree of mechanical softness, however, there can be problems related to cost and inhomogeneity of the materials.[11] Multilayer models hold a lot of promise for applications such as skin toxicology measurements,[12] however, they cannot be easily applied for more complex tissue or organ constructs including vasculature. Considerable attention has thus focused on the development of biocompatible scaffold materials for hosting cells in 3D. A variety of synthetic and bio-derived polymers (some resorbable, some not) have been used to mimic the ECM or connective tissue. In terms of technology integration, the major advances so far for 3D cell biology have been related to materials and methods used for scaffold preparation, and integration of microfabrication techniques, for example for fluidics. As might be expected, a challenge of 3D culture over 2D is associated with the difficulty of oxygenation of tissues in the absence of vasculature. Microfluidics have gained favor for a number of reasons, including for perfusion, reduction in reagent volumes, and the fact that flow induced stress

Prof. S. Inal, A. Hama, M. Ferro, Dr. C. Pitsalidis, Dr. D. Iandolo, A.-M. Pappa, Prof. R. M. Owens
Department of Bioelectronics
Ecole Nationale Supérieure des Mines
CMP-EMSE
Gardanne 13541, France
E-mail: sahika.inal@kaust.edu.sa; owens@emse.fr
Prof. S. Inal
Biological and Environmental Science and Engineering
King Abdullah University of Science and Technology (KAUST)
Thuwal 23955-6900, Kingdom of Saudi Arabia

**DOI: 10.1002/adbi.201700052**

Dr. J. Oziat, Dr. P. Mailley
CEA
LETI
MINATEC Campus
38054 Grenoble, France
M. Hadida, Dr. D. Marchat
Laboratoire Sainbiose
Ecole Nationale Supérieure des Mines
CIS-EMSE
St. Etienne 42023, France
Dr. M. Huerta
Department of Infectomics and Molecular Pathogenesis
Cinvestav 14-740, 070000, Mexico

 

is known to enhance differentiation via mechanotransduction and encourage intercellular/organ communication.[13,14] Excitingly, the latest trends have seen the integration of fluidics into 3D cultures made of polymeric scaffolds/hydrogels.[15] What appears to be missing, however, are techniques for evaluation of tissues. Optical techniques, that are the gold standard for monitoring cells cultured in 2D, can be challenging to apply in 3D due to difficulties in imaging through the scaffolds.[16] A significant challenge also relates to integration of other cell monitoring techniques and tools with 3D models, such as impedance spectroscopy and electrical transducers, frequently used to monitor barrier properties of epithelial and endothelial tissues.[17]

Electrical methods have a proven track record to be non-destructive and label-free for monitoring cells in real-time. Electrical methods for live-cell sensing refer to a broad range of measurements such as membrane potential probing,[18] impedance monitoring,[19] extracellular recordings from electrically active cells through both electrodes,[20] and transistors.[21] For non-electrogenic cells, electrical measurements can be used to evaluate cell coverage and differentiation, thus providing a measure of cell viability. Integrity of cell layers may be assessed by measuring the passive electrical resistance, known to alter after injury.[22] Certain issues such as the use of rigid, high impedance electronic materials like silicon oxide or gold, however, have meant that electronic monitoring of cells is not necessarily compatible with the push toward "softer" 3D materials that provide an improved interface and communication with biological systems.[23] Some progress has been made toward this goal: Esch et al.[24] have developed a "body on a chip" platform that incorporates gastrointestinal (GI) tract and liver 3D tissue with a pumpless microfluidic system used to perfuse cells. Integrated electrodes measured transepithelial resistance, but only of the GI cells which were cultivated in 2D on top of a porous membrane. 3D cell constructs have been monitored using vertical electrodes dipped into hydrogels containing spheroids.[25] Indeed, a number of reports have emerged in the past years using impedimetric methods to monitor 3D cultures, however, in all cases planar electrodes were used, implying that the tissues make non-conformal contact with the electrodes.[26,27] Matrix type gels trapping cells on top of microelectrode arrays enabled monitoring of cells for multiple days.[28,29] An advance on the 2D electrode system, is the use of four electrodes, for example in a microcavity array, increasing the feasibilty of the impedance technique for 3D cultures.[30,31] A recent study utilizes a microcavity array technology to assess the integrity of 3D spheroids in suspension, while maintaining the spheroid ultrastructure.[32]

Recently, a new generation of "smart" materials that can host cells in 3D has emerged. These materials integrate functionality into the hitherto "passive" scaffolds, while also solving the problem of rigidity of traditional 2D metal electrodes. Conducting polymers (CPs) are a prime example of such a material. Previously used in devices such as organic light-emitting diodes solar cells, and electrochromic devices, these materials have also been shown to bring enhanced capabilities to the interface with biology,[33–35] related in large part to their mechanical softness, mixed ionic/electronic conductivity as well as fabrication in nonstandard (nonplanar) conformable formats.[36] An added advantage is their optical transparency which allows for combined optical and electronic monitoring.[37–39] For 3D cell biology, the principal motivation for use of CPs as supports has been for the growth of electrically active cells (e.g. neurons) based on the idea that an electroactive material can modulate neuronal growth and differentiation and be used to engineer in vitro models of electro-responsive tissues.[40–42] A body of literature exists on CP-based hydrogels which have been shown to host cells, [43] some of these with the aim to provide an electrically conducting support material which can faciliate implanted neuronal constructs forming electroactive connections with the host tissue without provoking glial scarring.[44] Moreover, processibilty of poly(3,4-ethylenedioxythiophene) (PEDOT) has enabled preparation of conducting scaffolds/fibers comprising a variety of materials including bacterial cellulose.[45] However, these constructs are generally significantly more rigid than biological tissues, and tend to be brittle. Another approach has been the processing of CPs in the form of foams or sponges. Previous studies showed the generation of a biocompatible foam made of the CP poly(3,4-ethylenedioxythiophene):poly-(styrenesulfonate), (PEDOT:PSS).[46] These scaffolds not only successfully hosted mammalian cells, but also the cells within were shown to be responsive to the oxidation state of the conducting network. A composite of PEDOT and polyurethane has been reported to have high electrical conductivity and be mechanically robust, autoclavable and host cells, but has not yet been used for electrical stimulation or monitoring of 3D tissue.[47]

In this work, we employ an ice-templating (freeze casting) technique to fabricate PEDOT:PSS based scaffolds as the basis of a 3D living tissue-integrated electronic platform. The use of CP hydrogel-like scaffolds was chosen to generate highly efficient signal transduction due to an intimate and 3D contact of cells with the electroactive material. In contrast to previous studies with such porous materials, which do not actively utilize the electrical conductivity of the material or bias the scaffolds before (not during) cell culture,[46] the scaffolds presented here were prepared in situ within a device configuration. This allows us to perform electrical measurements during cell culture. Two key parameters were targeted for optimization in the current study to achieve efficient signal transduction; improving cell adhesion, and enhancing the conductivity of the scaffolds. Scaffolds were fabricated similarly to those previously reported,[46] with the key difference that two additives were used, collagen and dodecylbenzenesulfonic acid (DBSA), which improve cell adhesion and conductivity respectively, as will be detailed below.

We prepared scaffolds by freezing a pre-determined amount of an aqueous dispersion of PEDOT:PSS (with or without the additive), and a silane-based crosslinker, (3-glycidoxypropyl)-trimethoxysilane (GOPS), inside disposable cuvettes fixed on Au-coated substrates (**Figure 1**a). The dispersions inside the cuvettes were frozen at a controlled rate (0.9 °C $min^{-1}$), followed by the sublimation of the ice phase under high vacuum (see the Experimental section for details). As previously described,[46] the scaffolds are highly porous throughout the volume, with the exception of a "skin" layer formed on top of the scaffolds (Figure S1a, Supporting Information). The dimensions of the

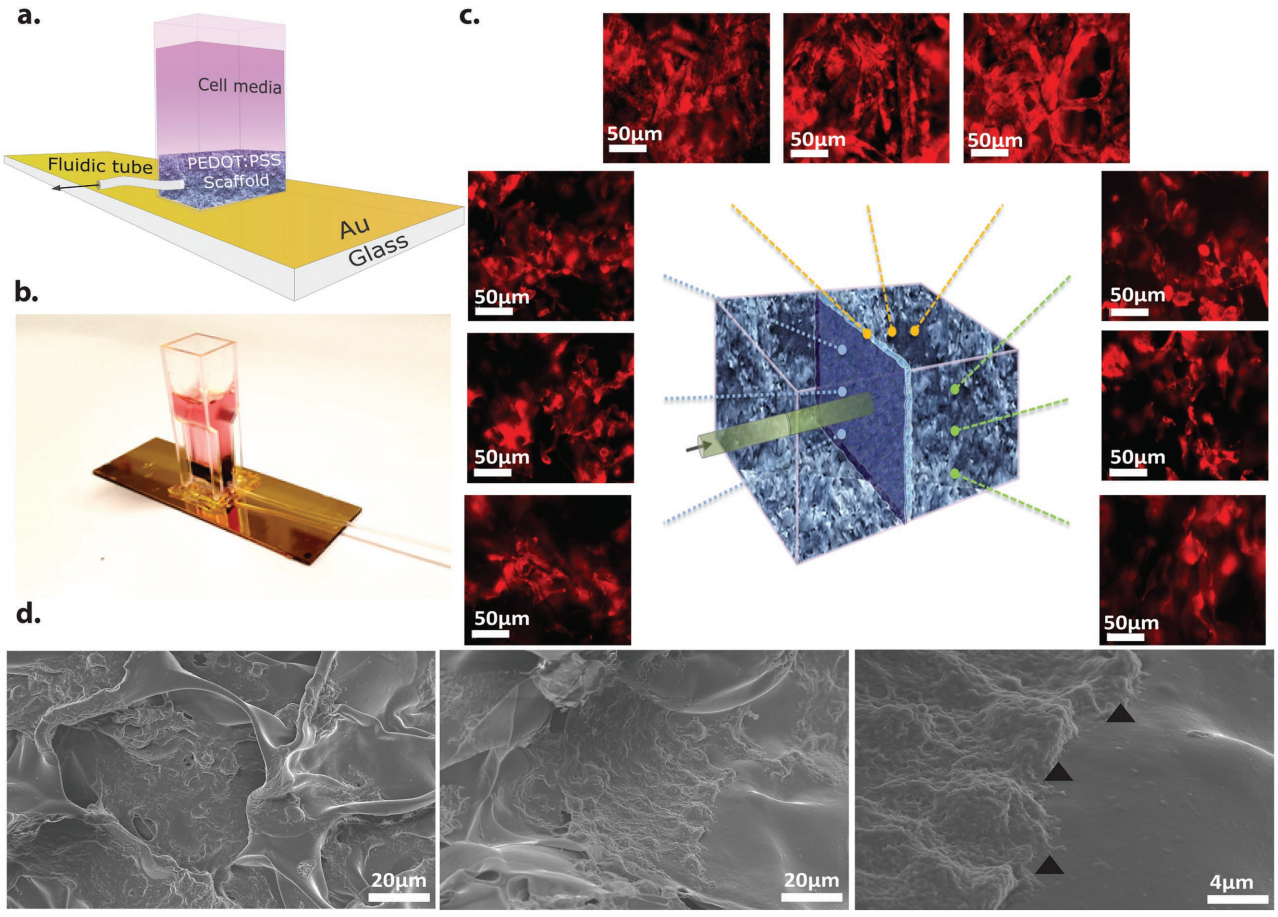


**Figure 1.** The design of 3D cell-integrated electronic platform. a) A schematic illustration and b) a photograph of the 3D CP scaffold showing the gold (Au) coated glass slide (used to provide electrical contact with the scaffold) and the integration of the media perfusion tube within the plastic cuvette used to contain the media. c) Fluorescence images of a collagen (0.05 wt%) containing scaffold seeded with MDCK II cells after 5 d of cell culture under continuous flow of media (1.6 μL $min^{-1}$). The central image illustrates the placement of the perfusion tube well into the center of the scaffold, while the surrounding pictures are immunofluorescence images taken from fixed sections of the scaffold showing labelled actin (stained with Rhodamine Phalloidin). The images show proliferation of cells within the scaffold. d) SEM images of a cell loaded collagen containing scaffold showing different areas (images taken from top of scaffold). Black arrows indicate the leading edge of cells growing over uncovered scaffold seen on the right side of the image (right).

scaffold are determined by the volume of the PEDOT:PSS dispersion and the geometry of the mold/cuvette. In the final structure, our scaffolds were designed to have dry dimensions of ≈10 × 4.5 × 1.5 mm (length × width × height). A typical scaffold prepared in a PDMS mold is shown in Figure S1b in the Supporting Information.

## 2. Assessing Cell Growth on PEDOT:PSS Scaffolds with Additives

The use of collagen as an additive was expected to improve cell adhesion and proliferation on the scaffolds for two reasons; reducing the mechanical stiffness of the scaffold by including a biopolymer, and also by virtue of the well-known role of collagen in cell adhesion. We included collagen (type I from rat tail) (0.05 wt%) in the PEDOT:PSS formulation before freeze drying. The mechanical properties of a scaffold used to host cells is known to be a determining parameter in dictating not only cell/material compatibility, but also cellular differentiation.[2] Collagen addition resulted in softer scaffolds, which we attributed to the water uptake capability and lower stiffness of the protein compared to the conjugated PEDOT backbone. (Figure S2a, Supporting Information). Collagen addition did not have any particular effect on pore size (Figure S2e–g, Supporting Information) compared to pristine scaffolds (Figure S2b–d, Supporting Information) with a good distribution of pores evident throughout. We expected such structures to be ideal for cell growth due to the high density of pores and their interconnection, allowing for fluid and gas uptake/release. Due to the challenge of maintaining a homogenous distribution and viability of cells inside a relatively large structure and to maximize the cell density and homogenize their attachment, we integrated media perfusion tubes inside the cuvettes (Figure 1a,b). We ensured that once the ice-templating process is complete, the opening of the tube corresponds approximately to the center of the scaffold. We seeded Madin Darby Canine Kidney (MDCK II) epithelial cells into collagen containing

scaffolds using a syringe to push and pull media through the perfusion tube to ensure access of cells to the entire scaffold. These cells were chosen as they have been well characterized in terms of their electrical properties using electrochemical impedance spectroscopy (EIS) techniques by us[37] and others on 2D planar electrodes, and known to have moderately high barrier properties.[48] The cells were pipetted onto the top of the scaffolds and the volume was sucked inside by the reverse flow applied through the fluidic tube. Upon seeding, fresh media was supplied through constant weak flow applied with a pump. Fluorescence images taken from different parts of the scaffold after 5 d of cell culture show that the perfusion aided homogenous population of the volume of the scaffold with cells rather than cells accumulating only at the surface (Figure 1c). In contrast, scaffolds prepared without the fluidics did not allow homogenous cell seeding throughout (Figure S3a, Supporting Information). Scanning electron microscopy (SEM) images (taken with a top-view) provide evidence for the presence of the cells covering the scaffolds—in some cases bare scaffold can still be seen with a leading edge of cells (Figure 1d (right)). Additional cross-sectional SEM images comparing scaffolds with and without cells, clearly show the presence of cells inside the scaffolds as both the smooth scaffold and the globular cell body and fibers can be identified (Figure S3b,c, Supporting Information).

## 3. Assessing Electrical Properties of PEDOT:PSS Scaffolds Before and After Cell Culture

As the cells cover the surface of the conducting scaffold, we expect to see changes in the electrochemical impedance spectrum, similar to electric cell–substrate impedance sensing performed with planar electrodes.[37,49] This would then allow for direct live-monitoring of the 3D cell culture. The electroactivity of the scaffolds was thus investigated by electrochemical impedance spectroscopy performed in culture media before and after 5 d of cell growth (**Figure 2**). Comparing the impedance of collagen containing scaffolds with cells, to those without cells, we can see that there is an increase in the magnitude of the impedance (Figure 2a) with a marked change in its phase, particularly at the low-to-mid frequency range of 0.1–100 Hz (Figure 2b). The magnitude of impedance at 1 Hz with cells ($|Z_{cells}| \approx 58$ kΩ) is double the value of that of the pristine scaffold ($|Z| \approx 28$ kΩ).

The impedance at the low frequency end of the spectrum is dominated typically by the electrode–media interface and at high frequencies by the culture medium appearing mostly as an ohmic flat line in the curve. For a 2D system, when cell layers cover the working electrode, additional contributions show up in the intermediate frequencies (≈100–1000 Hz).[49–51] The phase data display a new maximum at lower frequencies with

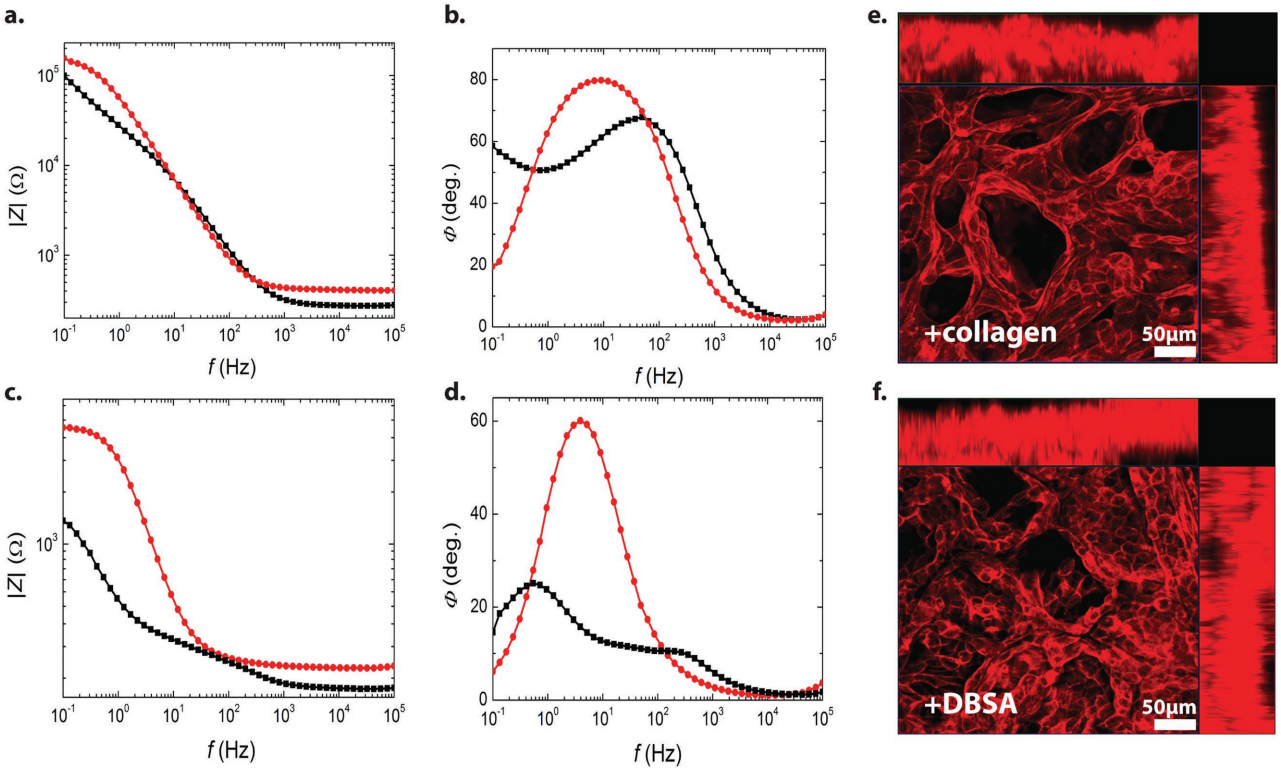


**Figure 2.** Comparison of a CP scaffold containing collagen or DBSA. Analysis of the a,c) magnitude and b,d) phase angle of the impedance of PEDOT:PSS scaffolds before and after growth of MDCK II LifeAct cells (expressing red fluorescent protein tagged actin). Black squares denote the spectrum of the bare scaffold, while red circles indicate the spectrum of the corresponding scaffold after cell seeding. The electrolyte is media that is renewed before measurements. Scaffolds were prepared with either a,b) 0.05 wt% collagen or with c,d) 0.5 wt% DBSA in the formulation. Cells were introduced into the scaffold and incubated for 5 d. Fluorescence orthoview of MDCK II LifeAct cells grown in scaffolds containing either e) collagen or f) DBSA. The images were taken after impedance measurements, using a confocal microscope.

an increased magnitude ($\Phi = 68°$; $\Phi_{cells} = 80°$), manifesting a capacitive component present in the circuit upon cell growth.[50] On planar PEDOT:PSS electrodes, increased phase values, albeit at the high frequency regime, arose due to growing cell layers on the electrodes, acting like a capacitive coating.[39] In line with similar EIS studies on planar electrodes,[52] the MDCK epithelial cells attaching to the walls of the scaffold act primarily as an insulating coating and thus impact the current flow within the material.

Inclusion of biopolymers such as collagen in the scaffold is expected to enhance the formation of tissues; however, this may come at the expense of electrical conductivity. Although the collagen containing scaffolds were postulated to be more cytocompatible, their ability to discriminate growth of the tissue on the scaffold via changes in impedance may not be sufficient. In an effort to render the scaffolds more conducting, we fabricated PEDOT:PSS scaffolds with the addition of the water soluble surfactant DBSA, known to increase conductivity in 2D thin film analogs of PEDOT:PSS.[53] DBSA has also been used as the primary dopant of PEDOT during its electropolymerization on metal surfaces.[54] We confirmed that the cells were distributed throughout the DBSA-containing scaffold thanks to our perfusion system (Figure S4, Supporting Information). As expected, DBSA containing scaffolds have significantly lower impedance at all low-to-intermediate frequencies compared to the collagen containing scaffolds of the same size as shown by the Bode plots (compare black squares in Figure 2a with Figure 2c). Comparing the two sets of data that belong to two different scaffolds (with collagen or with DBSA), we see that the cell-induced changes in the magnitude of impedance are magnified with the DBSA containing scaffold: a ≈6 times higher magnitude of impedance at 1 Hz when comparing the scaffold with ($|Z_{cells}| \approx 2900\ \Omega$) and without cells ($|Z| \approx 500\ \Omega$) (Figure 2c). The phase spectrum shows a marked change in the presence of cells with a new maximum of an increased value: the phase maximum increases from 25° to 60° in the presence of cells (Figure 2d). Similar changes in the electrochemical impedance properties of a metal electrode have been observed when an anti-myoglobin antibody bound to electrode surfaces, attributed to the insulating behavior of the protein, perturbing the electrode–electrolyte interface.[55] Overall, the frequency dependent impedance spectra of both types of scaffold exhibit features that are associated with the electrical sealing/blocking properties of the cell layer; however, with the presence of DBSA in the structure, these features are more prominent. Confocal images taken of MDCK II cells transfected with LifeAct TagRFP (red fluorescent protein tagged actin for live cell imaging) allow visualization of cells in both scaffold types, again confirming the excellent cell adhesion, and formation of contiguous sheets of cells around the walls of the scaffold (Figure 2e,f). We note the nondestructive nature of the EIS measurements which allows imaging to take place afterward. Movies of confocal *Z*-stack images for these samples are shown in Movie 1, Supporting Information (+collagen) and Movie S2, Supporting Information (+DBSA).

The experiments carried out with DBSA illustrate that for the design of such an electrical sensing platform, the initial conductivity of the scaffold used as the working electrode is crucial in order to broaden the sensitivity window for monitoring of cells. Remarkably, and perhaps as testimony to the robust nature of this particular cell type (MDCK II epithelial cells), the substitution of DBSA for collagen did not result in any noticeable changes in cell growth. We observed that the persistence of cells in the scaffolds containing DBSA was similar to collagen containing analogs. It is possible that there were changes in initial adhesion but we did not capture this since images were taken only at the end of the experiment. Besides high initial conductivity, a stable conductivity is also desirable. CPs may change their electrical properties over time due to alterations in the dopant content in their structure. This can be further promoted as they are exposed to complex aqueous environment such as cell media at an elevated temperature (37 °C). Control experiments carried out incubating the DBSA containing scaffolds in cell culture media for 7 d showed only negligible changes in conductivity, suggesting that there is not a significant loss of DBSA or other components from the scaffold (Figure S5, Supporting Information). This is also borne out by the continued growth of cells on the scaffolds, which do not appear to be adversely affected by the presence of DBSA or indeed the potential for its presence in the surrounding media. DBSA is a surfactant used in some cosmetics, therefore, cytotoxic effects may generally be those of a detergent which can be tolerated by cells at low concentrations.[56] The stability of the conductivity of DBSA-containing scaffolds speak to the excellent compositional properties of the scaffolds and their future application for longer-term monitoring of cell cultures.

## 4. Assessing Mechanical and Electrical Properties of PEDOT:PSS Scaffolds Containing DBSA and/or Collagen

The principle contribution of collagen, as an additive to the scaffolds, appears to be decreased mechanical rigidity, potentially resulting in less of a mismatch with tissue (reported mechanical properties of tissue vary significantly depending on the method used, but are generally considered to be in the low kPa range (1–100 depending on tissue type)).[2] The Young's modulus of pristine scaffolds was measured to be ≈45 kPa, while the collagen containing scaffolds were significantly softer, ≈6 kPa (**Figure 3**a) in agreement with previous reports on scaffolds of this type.[46]

While collagen improved mechanical properties of the pristine scaffolds, however, it appears to have decreased the suitability of the scaffolds for electrical monitoring. DBSA, on the other hand, lowered the impedance of the scaffolds and did not adversely affect cell growth. Improvement of conductivity upon addition of DBSA was confirmed in 3D scaffolds prepared outside the cuvette, in PDMS molds with identical volumes (Figure 3b). While the DBSA films are the most conducting, and collagen the least conducting, the combination of DBSA and collagen may be a good compromise. We therefore made a new generation of scaffold, this time with both collagen and DBSA. In the case of the collagen scaffolds we see the introduction of a circular arc in the low frequency regime that translates into a resistive component,[57] compared to the other scaffold types (Figure 3b, notice the smaller radius of semicircle of the

 

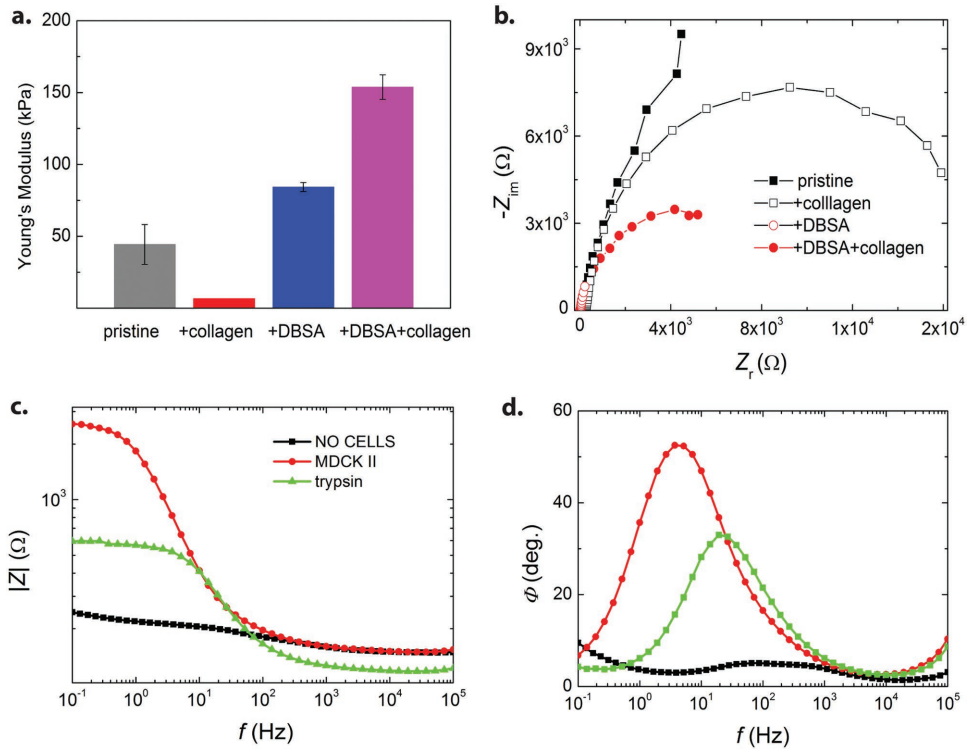


**Figure 3.** The second generation 3D CP scaffolds containing collagen and DBSA. a) Young's modulus of hydrated scaffolds prepared from a variety of compositions. The modulus was calculated from the slope of the linear part of the stress–strain curve, near zero strain (Figure S2a, Supporting Information). Error bars result from propagation taking into account at least two samples (for + collagen, $n = 1$). b) Impedance properties (the dependence of the real part ($Z_r$) and the imaginary part ($Z_{im}$) of complex impedance on the frequency, i.e., Nyquist plot) of a pristine PEDOT:PSS scaffold (black full squares), with collagen (0.05 wt%, black hollow squares), with DBSA (0.5 wt%, red hollow circles) and with DBSA and collagen (0.5 and 0.05 wt%, respectively, red circles). The samples were prepared in PDMS wells without the perfusion tube integrated into the structure (see Figure S1a in the Supporting Information for a photograph). c) The change in the magnitude, and d) in the phase angle of the impedance of a PEDOT:PSS scaffold containing 0.5 wt% of DBSA and 0.05 wt% of collagen before and after integration with MDCK II cells (black squares and red circles, respectively). The cell-loaded scaffold was exposed to trypsin on the fifth day (green triangles). The electrolyte is media that was freshly changed prior to measurements.

DBSA + collagen scaffold compared to collagen-only). While the DBSA scaffolds show the lowest impedance, the DBSA + collagen scaffolds represent a good middle ground. Surprisingly, inclusion of DBSA in the composition, negatively impacts the mechanical softness, resulting in more rigid scaffolds even than the pristine scaffolds (Figure 3a). These findings illustrate that additives in the polymeric mixtures do not have straightforward effects, and that phenomena such as phase-separation may be playing a role.

Again, we measured the impedance of the DBSA + collagen scaffolds before and after 5 d of cell growth (Figure 3c,d). These measurements confirm the suitability of these scaffolds for monitoring of tissue: we observe a clear increase in the magnitude of impedance at low frequencies (at 1 Hz, $|Z| \approx 30\ \Omega$ and $|Z_{cells}| \approx 1800\ \Omega$), and, as in the case of the DBSA-only scaffolds, the phase spectrum displays a new maximum at around 10 Hz with an increase in its magnitude in the presence of cells ($\Phi = 5°$ and $\Phi_{cells} = 50°$) (Figure 3c,d). We also evaluated the diffusion of a low molecular weight compound fluorescent tracer (Lucifer Yellow (LY), $M_w = 457.25$) through the scaffolds and confirmed that the capacity of the scaffolds for uptake of this molecule did not change significantly before or after cell culture (Figure S6, Supporting Information), indicating the ability of molecules to perfuse through the scaffolds. LY cannot penetrate into intact cells, and so must pass between cells or through the pores.[58] This assay also confirms the interconnectivity and mass diffusion through the scaffold. A further experiment with this generation of scaffolds aimed to remove the cells and to evaluate whether the impedance reverts back to its original properties. Trypsin is a well-known proteolytic enzyme which is routinely used in 2D cell culture to detach cells from polystyrene dishes. Although the LY assay showed diffusion of a small molecule through the scaffold, trypsin is a protein with a molecular weight of ≈24 kDa, thus its diffusion would be expected to be slower. Anticipating that interactions in a 3D tissue model would be significantly stronger than in 2D, a constant flow of the protease was applied to the cell-laden scaffolds for 1 h at 37 °C. After incubation, the impedance of the scaffolds was again measured. After trypsin treatment, the impedance magnitude at low frequencies decreases, e.g., from ≈1800 to ≈570 Ω measured at 1 Hz, while its phase has a lower magnitude (the peak at 50° drops to 33°) with its maximum shifted to higher frequencies (Figure 3c,d). Nyquist plots of the different scaffold types plus and minus cells clearly show the impact of the presence of cells on the scaffolds (Figure S7a–c, Supporting Information). The impact of trypsin is perhaps more evident in this

plot: the radius of the semi-circle is smaller when the cells are partially detached from the scaffold, pointing to a decrease in the impedance of the system (Figure S7c, Supporting Information). We posit that although the cells may have detached, they were only partially removed from the scaffold despite extensive washing. Additionally, remaining extracellular matrix deposited by the cells may contribute to the increase of impedance.

## 5. Suitability of PEDOT:PSS Scaffolds for Co-Culture of Fibroblasts and Epithelial Cells

As a final test of the feasibility of our platform for use in generating tissue-like structures in vitro, we proceeded to test the adhesion and growth of multiple cell types. Two types of cells were chosen; human telomerase immortalized fibroblasts cells (TIF) transfected with the LifeAct plasmid, and MDCK II cells transfected with an eGFP plasmid. The transfections allow visualization of the TIF (red) and the MDCK II cells (green) simultaneously. The fluorescence and SEM images (**Figure 4**a,b) reveal that PEDOT:PSS scaffolds provide a suitable 3D environment for co-culture of both cell types. In order to optimize the seeding of both cells types, fibroblasts were seeded first throughout the scaffold and incubated for 1 h. Then, epithelial cells were added to form an "epithelial layer."

These two complementary cell types were used to represent an "in vivo like" tissue structure; fibroblasts, as nonadhesive cells (with respect to the cell-cell junction), are found deep inside the tissue. They are responsible for the secretion of extracellular matrix allowing the remodeling of cell environment to be suitable for the subsequent formation of an epithelial layer (the MDCK cells). In our case, we expect a self-organization of both cell types and a remodeling of the scaffold. The fluorescence images illustrate clearly the dispersion of both cell types within the scaffold. In the SEM images, we can appreciate the different morphologies of the cells. In Figure 1c,d, we saw that the epithelial cells were forming sheets or monolayers on the scaffold surface. In the images shown in Figure 4, we see evidence of cells spanning the pores, or perhaps projecting extracellular matrix fibers across, which we posit to be the fibroblasts forming a "connective" tissue like structure. This "tissue like" auto-organization is highly promising for generating physiologically relevant tissue. The 3D scaffold infiltrated by cells herein can now be envisaged as a bioelectronic device that enables electronic, label-free sensing of cells. Here, the conducting polymer performs two distinct functions: (1) housing for cell culture with 3D physical contacts with cells, (2) "soft" electrode function allowing for monitoring of the presence of cells. Such scaffold-engineered living electrodes can be an alternative platform measuring cell viability against toxic components in cell environments.

## 6. Conclusions

In this work, we demonstrate for the first time the use of a 3D PEDOT:PSS-based scaffold with a dual purpose—to both host and monitor cells. In contrast to more traditional 3D scaffolds using passive materials as a mechanical support, the CP provides a new functionality thanks to its electroactivity. We show the preperation of different scaffolds simply by blending additives with the CP dispersion, allowing for tunability of different properties of the scaffolds, including mechanical stiffness (collagen) and conductivity (DBSA). Moreover, a simple perfusion system was used to ensure homogenous growth of cells throughout the scaffolds. Extensive tissue formation was clear at multiple days after seeding. Although the addition of collagen was not found to be essential in the case of MDCK II cell growth, the scaffolds containing collagen were softer than the pristine ones. The stiffness of the latter scaffolds approaches the stiffness of the biological tissue and its tunability holds great promise for engineering scaffolds with mechanical properties tailored for building specific tissue types. Current work is focusing on optimizing blends of collagen and DBSA to enhance both electrical and mechanical properties. Future work with other cell types requiring coating with ECM-like proteins such as collagen will benefit from this knowledge. Current studies focus on ascertaining the molecular distribution of the collagen versus the CP within the scaffold architecture, as it is highly possible that the additives are not exposed on the surface but rather contained within the bulk. Another focus is on modelling the changes in the complex impedance spectrum of the 3D scaffolds due to cell growth and understanding the different contributions of the resistance and capacitance of cells to the spectra in order to quantify cell coverage.

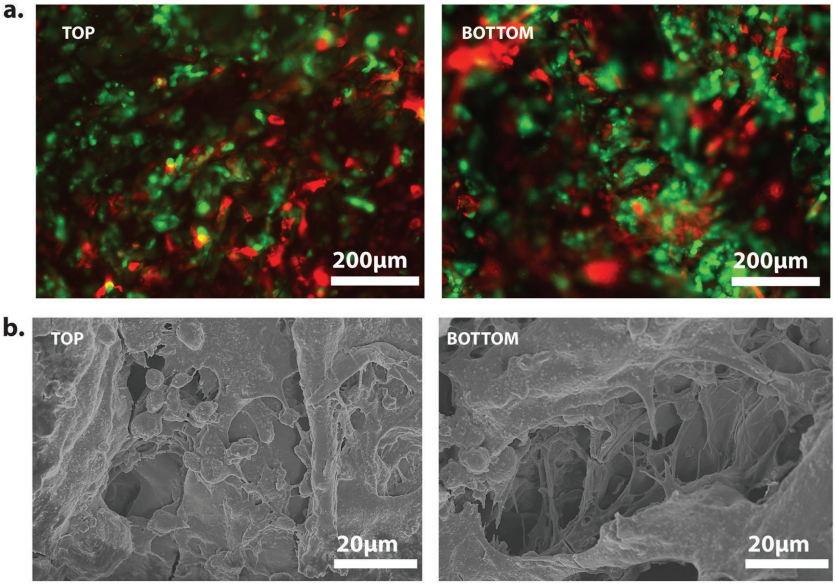


**Figure 4.** PEDOT:PSS scaffolds for co-culture of fibroblasts and epithelial cells. a) Confocal images and b) SEM images of co-culture of MDCK II eGFP (green) and TIF lifeAct (telomere immortalized fibroblasts, red) cells cultured inside a PEDOT:PSS based scaffold (collagen 0.05 wt%). The images confirm that cells adhered therein, organized, and survived for 5 d.

## 7. Experimental Section

*Preparation of the 3D CP Platform*: Scaffolds were fabricated from an aqueous dispersion of PEDOT:PSS (Clevios PH-1000, Heraeus) at a concentration of 1.25 wt%, with GOPS (Sigma-Aldrich) added as a crosslinker (3 wt%) to improve mechanical robustness and stability in water. This formulation was used for all the scaffolds and denoted as "pristine" scaffolds. For modified scaffolds, the PEDOT:PSS/GOPS dispersion was mixed with collagen (0.05 wt%, type I from rat tail) and/or with DBSA (0.5 wt%). The scaffolds to be used for electrical measurements were prepared in disposable semi-micropolystyrene cuvettes (Sigma Aldrich) with maximum filling volume of 3 mL. These cuvettes were modified such that a plastic tubing (0.72 mm inner diameter and 1.22 mm outer diameter) was incorporated. Once the tubes were fixed on the cuvettes, they were placed with a medical glue on top of Au (150 nm) coated glass substrates. The PEDOT:PSS dispersion was poured into these customized molds, at a volume of ≈250 µL, ensuring that the tube was covered by the polymer dispersion. The samples were then placed in a freeze-dryer (Cryotec), where they were frozen from 5 to –40 °C at a controlled rate of –0.9 °C $min^{-1}$, at which point the ice phase was sublimed from the scaffolds, as described by Wan et al.[46]

Following sublimation, the scaffolds were baked at 50 °C for 3 h. The resulting scaffolds had a dry volume of 10 × 4.5 × 1.5 $mm^3$ (length × width × height), where the height was adjusted by the added volume of the dispersion and the width and length were predetermined by the inner dimensions of the cuvette. In this work, before performing any of the reported experiments, all scaffolds were rinsed with deionized (DI) water multiple times using the perfusion tube. They were then kept in DI water over 24 h to enable the diffusion of low molecular components out of the structure. The scaffolds that were used for cell culture experiments were further treated with ethanol (70 vol%) for about 30 min for sterilization purposes.

*Scaffold Characterization*: Scaffold microstructure was characterized using SEM. SEM (MEB Ultra 55- Carl ZEISS) was specifically used to evaluate the invasion of cells into the scaffolds. Briefly, cells in the scaffold were fixed in 4% paraformaldehyde for 20 min under perfusion at room temperature, followed by extensive washing with phosphate buffered saline (PBS). The scaffold was then detached from the glass for dehydration in a graded ethanol series. Finally, the sample was coated with 10 nm Gold/Paladium and analyzed at 5 kV power.

The compressive modulus of hydrated PEDOT-based scaffolds was measured using an Instron with a 1 kN load cell. Each scaffold was immersed for 1 h in PBS and then tested. The samples were compressed at a speed of 1 mm $s^{-1}$. The Young's modulus was calculated as the slope in the linear part of the strain stress curve.

For the diffusion experiments, LY (Sigma Aldrich, $M_w$ = 457.25 Da) was used as a model fluorescent tracer. Briefly, the plastic cuvettes containing the scaffolds were incubated in a 900 × $10^{-6}$ M solution of LY in Hank's balanced salt solution (HBSS) to a volume of 1 mL and left overnight. The injection of the solution was via the tubing inside the scaffold, in a similar manner to the media and cell seeding procedure. Following incubation, the solution was removed and substituted by a fresh HBSS solution of same volume. At predetermined time points, ($t$ = 0, 30, 60, 120, 240, and 480 min) 20 µL of the solution was removed. The collected samples were transferred to a 96 well plate and measured in a UV spectrophotometer (TECAN, Infinite M1000) at 435 nm.

*Cell Culture Experiments*: MDCK II cells (a gift from Frederic Luton (IPMC, Valbonne)) were cultured in DMEM low glucose supplemented with 10% fetal bovine serum, 2 × $10^{-3}$ M glutamine, 50 U $mL^{-1}$ penicillin, 50 µg $mL^{-1}$ streptomycin. TIF cells were kindly provided by Ellen Van Obergghen Schilling (iBV Valrose, Nice). TIF LifeAct were prepared for this study in the same manner according to the manufacturer's guidelines (Ibidi, GmbH) and as described previously[37] using pCMVLifeAct–TagRFP. To keep pressure on the fluorescent actin expression, 500 µg $mL^{-1}$ of Geneticin were added to the media. 5 mL of 3 × $10^6$ MDCK II cells in suspension were perfused through the scaffold using the same media supplemented with 20 × $10^{-3}$ M 4-(2-hydroxyethyl)-1-piperazineethane sulfonic acid (HEPES) +/– geneticin as appropriate. Cells were seeded on top of the scaffold and slowly withdrawn through the fluidic until a thin layer of liquid was observed on the scaffold surface. After cell seeding, the scaffolds were incubated for 1 h at 37 °C to allow the cells to adhere, after which fresh media was added to the cuvettes to remove non adherent cells. A plastic lid was placed on the cuvette to ensure sterility. A weak flow of 1.6 µL $min^{-1}$ was applied to perfuse the cells for 5 d and the samples were incubated in humidified atmosphere at 37 °C and 5% $CO_2$.

For the trypsin experiment, the scaffolds were washed several times with PBS to remove the media. Then PBS solution was replaced by a solution containing 0.25% trypsin and a constant flow of 10 µL $min^{-1}$ was applied to help the dissociation of the cells for 1 h at 37 °C. After the incubation, several manual cycles of perfusion/withdrawal were applied to the scaffold to remove the cells.

For the co-culture, MDCK II eGFP (gift from Frederic Luton) was cultured in the same media as MDCK II cells. TIF pLifeACT were cultured in the same media as MDCKII cells with a supplement of 50 µg $mL^{-1}$ of Geneticin added in the media. Cells were grown in the scaffold using the same media supplemented with 20 × $10^{-3}$ M HEPES. 3 mL of 7 × $10^5$ TIF pLifeACT cells were seeded on top of the scaffold and slowly withdrawn and then perfused in order to maximize the number of cells inside the scaffold. After incubation at 37 °C for 1 h, the scaffold was perfused by fresh media in order to remove nonattached cells and then 3 mL of 3 × $10^6$ MDCK II GFP cells were seeded. In this case, media was only withdrawn to enable the penetration of cells. After incubation at 37 °C for 1 h, the scaffold was perfused by fresh media again to remove remaining nonattached cells. A flow of 25 µL $min^{-1}$ was applied to perfuse the scaffold during the 5 d of cell culture, when the media was recycled in order to supply secreted growth factors. A higher flow rate was used for the co-culture compared to the monoculture to ensure nutrient delivery to the greater number of cells.

*Immunofluorescent Staining*: MDCK II cells were fixed in 4% paraformaldehyde for 20 min and permeabilized using 0.1% Triton X-100 for 10 min at room temperature. The scaffolds were washed extensively with PBS and incubated with Rhodamine Phalloidin and DAPI (Invitrogen) for 30 min to label actin and the nuclei, respectively. The scaffold was monitored under epifluorescence/confocal microscope (AxioObserver Z1 LSM 800 ZEISS).

*Electrical Characterization of Scaffolds*: Impedance spectra of the scaffold/cell culture platform were measured using an Autolab potentiostat equipped with a frequency response analysis module. Commercially available Ag/AgCl electrode and a platinum mesh (45 mm × 25 mm) immobilized inside the cuvettes were used as the reference and counter electrodes, respectively. The counter electrode was sufficiently large in order to have minimal contribution on the impedance values measured. The applied AC voltage was 0.01 V and measurements were taken at a DC potential corresponding to the open circuit potential against the reference electrode. The electrolyte solution was the cell culture medium that was refreshed before each measurement, unless otherwise stated.

## Supporting Information

Supporting Information is available from the Wiley Online Library or from the author.

## Acknowledgements

S.I. and C.P. gratefully acknowledge financial support from the ANR 3Bs project. This work was also supported by the Marie Curie ITN project OrgBio No. 607896. S.I. and A.H. benefitted from fruitful discussions with Professor Gordon Wallace at the University of Wollongong thanks to visits funded by the Marie Curie MASK project No. 269302, and from Dr. Pierre Leleux (EMSE) and Dr. Ilke Uguz (EMSE) related to device fabrication.

 

## Conflict of Interest

The authors declare no conflict of interest.

## Keywords

3D cell culture, biosensors, cell culture, conducting polymers, scaffolds

Received: March 3, 2017
Revised: March 30, 2017
Published online: May 3, 2017

[1] D. E. Discher, P. Janmey, Y. L. Wang, *Science* **2005**, *310*, 1139.
[2] A. J. Engler, S. Sen, H. L. Sweeney, D. E. Discher, *Cell* **2006**, *126*, 677.
[3] B. M. Baker, C. S. Chen, *J. Cell Sci.* **2012**, *125*, 3015.
[4] J. Barrila, A. L. Radtke, A. Crabbé, S. F. Sarker, M. M. Herbst-Kralovetz, C. M. Ott, C. A. Nickerson, *Nat. Rev. Microbiol.* **2010**, *8*, 791.
[5] M. L. Li, J. Aggeler, D. A. Farson, C. Hatier, J. Hassell, M. J. Bissell, *Proc. Natl. Acad. Sci. USA* **1987**, *84*, 136.
[6] C. D. Roskelley, P. Y. Desprez, M. J. Bissell, *Proc. Natl. Acad. Sci. USA* **1994**, *91*, 12378.
[7] E. Urich, C. Patsch, S. Aigner, M. Graf, R. Iacone, P.-O. Freskgård, *Sci. Rep.* **2013**, *3*, 1500.
[8] E. R. Shamir, A. J. Ewald, *Nat. Rev. Mol. Cell Biol.* **2014**, *15*, 647.
[9] M. Huerta, J. Rivnay, M. Ramuz, A. Hama, R. M. Owens, *APL Mater.* **2015**, *3*, 030701.
[10] L. Ylä-Outinen, T. Joki, M. Varjola, H. Skottman, S. Narkilahti, *J. Tissue Eng. Regener. Med.* **2014**, *8*, 186.
[11] C. S. Hughes, L. M. Postovit, G. A. Lajoie, *Proteomics* **2010**, *10*, 1886.
[12] F. Netzlaff, C.-M. Lehr, P. W. Wertz, U. F. Schaefer, *Eur. J. Pharm. Biopharm.* **2005**, *60*, 167.
[13] J. Shemesh, I. Jalilian, A. Shi, G. Heng Yeoh, M. L. Knothe Tate, M. Ebrahimi Warkiani, *Lab Chip* **2015**, *15*, 4114.
[14] S. Halldorsson, E. Lucumi, R. Gómez-Sjöberg, R. M. T. Fleming, *Biosens. Bioelectron.* **2015**, *63*, 218.
[15] Y. Shin, S. Han, J. S. Jeon, K. Yamamoto, I. K. Zervantonakis, R. Sudo, R. D. Kamm, S. Chung, *Nat. Protoc.* **2012**, *7*, 1247.
[16] B. W. Graf, S. A. Boppart, in *Live Cell Imaging* (Ed.: D. B. Papkovsky), Humana Press, Totowa, NJ, **2010**, pp. 211–227.
[17] A. Herland, A. D. van der Meer, E. A. FitzGerald, T.-E. Park, J. J. F. Sleeboom, D. E. Ingber, *PLoS ONE* **2016**, *11*, e0150360.
[18] C. D. McCaig, A. M. Rajnicek, B. Song, M. Zhao, *Physiol. Rev.* **2005**, *85*, 943.
[19] I. Giaever, C. R. Keese, *Proc. Natl. Acad. Sci. USA* **1984**, *81*, 3761.
[20] M. E. Spira, A. Hai, *Nat. Nanotechnol.* **2013**, *8*, 83.
[21] P. Fromherz, A. Offenhäusser, T. Vetter, J. Weis, *Science* **1991**, *252*, 1290.
[22] I. Giaever, C. R. Keese, *Nature* **1993**, *366*, 591.
[23] X. Cui, V. A. Lee, Y. Raphael, J. A. Wiler, J. F. Hetke, D. J. Anderson, D. C. Martin, *J. Biomed. Mater. Res.* **2001**, *56*, 261.
[24] M. B. Esch, H. Ueno, D. R. Applegate, M. L. Shuler, *Lab Chip* **2016**, *16*, 2719.
[25] S.-M. Lee, N. Han, R. Lee, I.-H. Choi, Y.-B. Park, J.-S. Shin, K.-H. Yoo, *Biosens. Bioelectron.* **2016**, *77*, 56.
[26] K. F. Lei, Z.-M. Wu, C.-H. Huang, *Biosens. Bioelectron.* **2015**, *74*, 878.
[27] M. Frega, M. Tedesco, P. Massobrio, M. Pesce, S. Martinoia, *Sci. Rep.* **2014**, *4*, DOI: 10.1038/srep05489.
[28] S.-P. Lin, T. R. Kyriakides, J.-J. J. Chen, *Biomaterials* **2009**, *30*, 3110.
[29] T. A. Nguyen, T.-I. Yin, D. Reyes, G. A. Urban, *Anal. Chem.* **2013**, *85*, 11068.
[30] D. Kloß, R. Kurz, H.-G. Jahnke, M. Fischer, A. Rothermel, U. Anderegg, J. C. Simon, A. A. Robitzki, *Biosens. Bioelectron.* **2008**, *23*, 1473.
[31] D. Kloß, M. Fischer, A. Rothermel, J. C. Simon, A. A. Robitzki, *Lab Chip* **2008**, *8*, 879.
[32] S. Poenick, H.-G. Jahnke, M. Eichler, S. Frost, H. Lilie, A. A. Robitzki, *Biosens. Bioelectron.* **2014**, *53*, 370.
[33] J. Rivnay, M. Ramuz, P. Leleux, A. Hama, M. Huerta, R. M. Owens, *Appl. Phys. Lett.* **2015**, *106*, 043301.
[34] A. Jonsson, S. Inal, I. Uguz, A. J. Williamson, L. Kergoat, J. Rivnay, D. Khodagholy, M. Berggren, C. Bernard, G. G. Malliaras, D. T. Simon, *Proc. Natl. Acad. Sci. USA* **2016**, *113*, 9440.
[35] J. Rivnay, R. M. Owens, G. G. Malliaras, *Chem. Mater.* **2014**, *26*, 679.
[36] D. Khodagholy, T. Doublet, P. Quilichini, M. Gurfinkel, P. Leleux, A. Ghestem, E. Ismailova, T. Herve, S. Sanaur, C. Bernard, G. G. Malliaras, *Nat. Commun.* **2013**, *4*, 1575.
[37] M. Ramuz, A. Hama, J. Rivnay, P. Leleux, R. M. Owens, *J. Mater. Chem. B* **2015**, *3*, 5971.
[38] M. Ramuz, A. Hama, M. Huerta, J. Rivnay, P. Leleux, R. M. Owens, *Adv. Mater.* **2014**, *26*, 7083.
[39] S. Löffler, A. Richter-Dahlfors, *J. Mater. Chem. B* **2015**, *3*, 4997.
[40] C. E. Schmidt, V. R. Shastri, J. P. Vacanti, R. Langer, *Proc. Natl. Acad. Sci. USA* **1997**, *94*, 8948.
[41] N. Bhagwat, K. L. Kiick, D. C. Martin, *J. Mater. Res.* **2014**, *29*, 2835.
[42] K. J. Gilmore, M. Kita, Y. Han, A. Gelmi, M. J. Higgins, S. E. Moulton, G. M. Clark, R. Kapsa, G. G. Wallace, *Biomaterials* **2009**, *30*, 5292.
[43] D. Mawad, A. Artzy-Schnirman, J. Tonkin, J. Ramos, S. Inal, M. M. Mahat, N. Darwish, L. Zwi-Dantsis, G. G. Malliaras, J. J. Gooding, A. Lautor, M. M. Stevens,*Chem. Mater.* **2016**, *28*, 6080.
[44] R. A. Green, K. S. Lim, W. C. Henderson, R. T. Hassarati, N. H. Lovell, in *35th Annual International Conference of the IEEE Engineering in Medicine and Biology Society (EMBC)* **2013**, 6957.
[45] C. Chen, T. Zhang, Q. Zhang, Z. Feng, C. Zhu, Y. Yu, K. Li, M. Zhao, J. Yang, J. Liu, D. Sun, *ACS Appl. Mater. Interfaces* **2015**, *7*, 28244.
[46] A. M.-D. Wan, S. Inal, T. Williams, K. Wang, P. Leleux, L. Estevez, E. P. Giannelis, C. Fischbach, G. G. Malliaras, D. Gourdon, *J. Mater. Chem. B* **2015**, *3*, 5040.
[47] M. Sasaki, B. C. Karikkineth, K. Nagamine, H. Kaji, K. Torimitsu, M. Nishizawa, *Adv. Healthcare Mater.* **2014**, *3*, 1919.
[48] J. Wegener, C. R. Keese, I. Giaever, *Exp. Cell Res.* **2000**, *259*, 158.
[49] S. Arndt, J. Seebach, K. Psathaki, H.-J. Galla, J. Wegener, *Biosens. Bioelectron.* **2004**, *19*, 583.
[50] V. Atanasov, N. Knorr, R. S. Duran, S. Ingebrandt, A. Offenhäusser, W. Knoll, I. Köper, *Biophys. J.* **2005**, *89*, 1780.
[51] A. S. Karimullah, D. R. S. Cumming, M. Riehle, N. Gadegaard, *Sens. Actuators B Chem.* **2013**, *176*, 667.
[52] C. M. Lo, C. R. Keese, I. Giaever, *Biophys. J.* **1995**, *69*, 2800.
[53] S. Zhang, P. Kumar, A. S. Nouas, L. Fontaine, H. Tang, F. Cicoira, *APL Mater.* **2015**, *3*, 014911.
[54] A. R. Harris, P. J. Molino, R. M. I. Kapsa, G. M. Clark, A. G. Paolini, G. G. Wallace, *Analyst* **2015**, *140*, 3164.
[55] S. K. Mishra, A. K. Srivastava, D. Kumar, Rajesh , *RSC Adv.* **2014**, *4*, 21267.
[56] L. C. Becker, W. F. Bergfeld, D. V. Belsito, R. A. Hill, C. D. Klaassen, D. C. Liebler, J. G. Marks, R. C. Shank, T. J. Slaga, P. W. Snyder, F. A. Andersen, *Int. J. Toxicol.* **2010**, *29*, 288S.
[57] E. Stavrinidou, M. Sessolo, B. Winther-Jensen, S. Sanaur, G. G. Malliaras, *AIP Adv.* **2014**, *4*, 017127.
[58] S. A. Tria, L. H. Jimison, A. Hama, M. Bongo, R. M. Owens, *Biochim. Biophys. Acta* **2013**, *1830*, 4381.

 